

States of ^{38}S from the $^{36}\text{S}(t,p)^{38}\text{S}$ reaction

N. J. Davis, J. A. Kuehner, A. A. Pilt, A. J. Trudel, M. C. Vetterli, and C. Bamber
McMaster University, Hamilton, Ontario, Canada L8S 4K1

E. K. Warburton and J. W. Olness
Brookhaven National Laboratory, Upton, New York 11973

S. Raman
Oak Ridge National Laboratory, Oak Ridge, Tennessee 37831
 (Received 19 April 1985)

The $^{36}\text{S}(t,p)^{38}\text{S}$ reaction was studied at 18-MeV bombarding energy with an overall energy resolution of 55 keV. Excited states of ^{38}S were identified at energies (uncertainties in parentheses) of 1295(10), 2835(14), 3375(17), 3690(17), 4336(20), 4478(22), 4955(25), 5064(27), 5278(28), 6000(30), and 6605(60) keV. Angular distributions were measured for protons leading to the ground state and ten lowest excited states. The data are compared with distorted-wave Born approximation calculations in which a microscopic two-nucleon form factor was employed. On this basis spin assignments have been made for several states. A comparison is made between levels observed in ^{38}S and those predicted by the weak coupling and shell models.

I. INTRODUCTION

The (t,p) reaction is particularly useful for populating states in neutron rich nuclei. For even-even nuclei, the target spin is zero and the determination of spins can be carried out unambiguously by comparison of the experimental proton angular distributions with DWBA calculations. Angular distributions from (t,p) reactions have been used previously to determine level spins for nuclei in the upper *sd* shell.¹⁻³ In addition, (t,p γ) angular correlation studies have provided a method for spin determinations.⁴⁻⁶ In their $^{32}\text{S}(t,p)^{34}\text{S}$ study, Crozier *et al.*³ include shell model calculations for ^{34}S which show that in this region of the *sd* shell, the predicted energy levels are in good agreement with experiment below 5 MeV. Nuclei in the *fp* shell have also been studied using (t,p) reactions.⁷⁻¹¹ Shell model calculations are more difficult for these nuclei and ideally a large configuration space should be used. Casten *et al.*¹² have studied $L=0$ transitions for the (t,p) reaction to isotopes of Ti, Cr, and Fe. They showed that the magnitudes of calculated differential cross sections are sensitive to small proportions of transferred two-neutron configurations other than $(1f_{7/2})^2$ included in the DWBA form factor.

^{38}S is an interesting nucleus because, from the simplest shell model view, there are only two neutrons outside the closed neutron *sd* shell. Therefore, energy levels populated by the (t,p) reaction are expected to be largely two-neutron configurations, with protons not playing an important role in the reaction.

There is very little previous knowledge about the excited states of ^{38}S . This is because ^{38}S is a neutron-rich nucleus that cannot be populated by the commonly used reactions on readily available targets. ^{36}S has a very low natural abundance, so targets of this isotope are rare and have not been used previously with the (t,p) reaction.

However, states at 1280(40) and 3380(100) keV have been measured by Fifield *et al.*¹³ in the two-proton pickup reaction $^{40}\text{Ar}(^{11}\text{B},^{13}\text{N})^{38}\text{S}$. States in ^{38}S have also been observed in the $^{36}\text{S}(^{14}\text{C},^{12}\text{C})^{38}\text{S}$ and $^{36}\text{S}(^{18}\text{O},^{16}\text{O}\gamma)^{38}\text{S}$ reactions studied by Mayer *et al.*¹⁴ For the $(^{18}\text{O},^{16}\text{O}\gamma)$ reaction two strong peaks were observed in the γ -ray spectrum measured in coincidence with light particles, from which energies for the first and second excited states of ^{38}S of 1296.2(4) and 2834.4(7) keV were assigned. Additional ^{38}S states were observed in their ^{12}C and ^{16}O particle spectra and assigned energies of 3.71, 4.43, and 6.02 MeV.

II. EXPERIMENTAL PROCEDURE

The $^{36}\text{S}(t,p)^{38}\text{S}$ reaction was studied using an 18-MeV beam of tritons from the McMaster University tandem accelerator. The target was prepared¹⁵ by completely sulfiding a 200- $\mu\text{g cm}^{-2}$ silver foil, using sulfur enriched to 81.1(0.2)% in ^{36}S , the remaining 18.8(0.2)% being ^{34}S . Other known contaminants¹⁶ in the target are trace amounts of B, Na, Al, Si, and K. The net quantity of ^{36}S in the target was estimated as 23.0(3.4) $\mu\text{g cm}^{-2}$, while the ^{34}S content was 5.0(0.8) $\mu\text{g cm}^{-2}$. Silver was used in the target since it is very reactive with sulfur, resulting in very little of the target material being lost during manufacture. Unfortunately, however, the silver causes a significant background in the spectra, and contributes also to some loss of energy resolution.

A delay-line gas counter placed in the focal plane of an Enge split-pole magnetic spectrograph was used to detect protons from the (t,p) reaction. The position along the focal plane and the energy loss in the gas counter were measured, while a scintillator placed behind the delay line counter was used to measure the total energy of the particles. The detector was calibrated by changing the magnet-

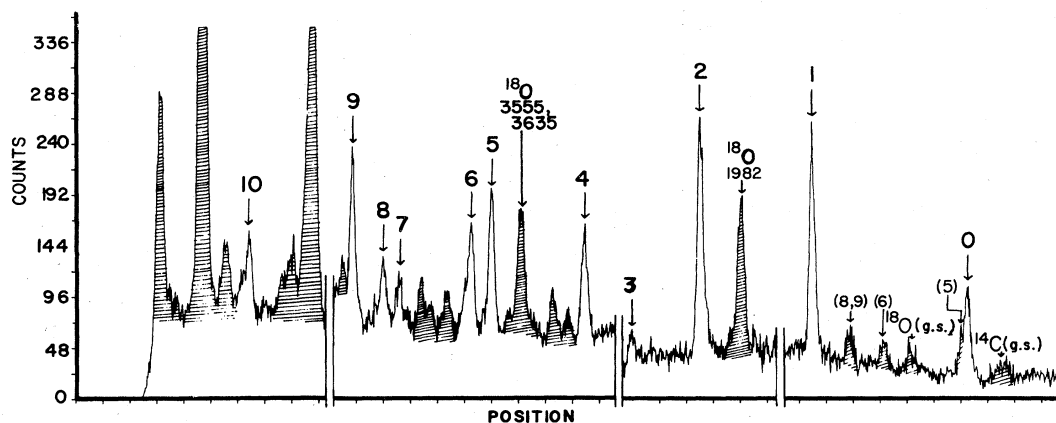


FIG. 1. Proton spectrum from the $^{36}\text{S}(t,p)^{38}\text{S}$ reaction measured at $\theta_p=20^\circ$. States of ^{38}S are labeled 0–10 corresponding to the excitation energies given in Table I. For states of ^{36}S from the contaminant $^{34}\text{S}(t,p)^{36}\text{S}$ reaction the state numbers are indicated in parentheses. The other shaded peaks are states of higher excitation in ^{36}S and states arising from components of the target other than ^{36}S .

ic field to move the peak of the $^{12}\text{C}(t,p)^{14}\text{C}(\text{g.s.})$ reaction to a number of positions along the focal plane. Protons were selected from the full position spectrum by setting a two-dimensional gate on the position versus total energy spectrum. The overall energy resolution in the proton spectrum was 55 keV. A typical spectrum, taken at 20° , is shown in Fig. 1. Because of the significant amount of ^{34}S in the target, it was necessary to measure additional spectra using an enriched ^{34}S target for comparison. The shaded peaks in Fig. 1 have been identified as arising from ^{34}S , ^{16}O , and ^{12}C contaminants.

III. ENERGY LEVELS IN ^{38}S

Excitation energies of states in ^{38}S were measured by calculating energy differences between protons corresponding to adjacent states in ^{38}S . Because of slight nonuniformities in the energy calibration across the counter, differences in excitation energies are measured more accurately than absolute energies. Excitation energy differences were found by taking a mean of values calculated from the proton energies at angles for which the

TABLE I. Excitation energies and spin and parity assignments for states in ^{38}S . Our results yield the value $Q_0=3838(30)$ keV for the $^{36}\text{S}(t,p)^{38}\text{S}$ ground state Q value.

State number	Energy (keV)	J^π
0	0	0^+
1	1295(10)	2^+
2	2835(14)	4^+
3	3375(17)	$2^+(1^-)$
4	3690(17)	$5^-, 6^+$
5	4336(20)	$4^+(3^-)$
6	4478(22)	$3^-, 4^+$
7	4955(25)	$2^+(1^-, 3^-)$
8	5064(27)	$3^-(2^+)$
9	5278(28)	$2^+(1^-, 3^-)$
10	6000(30)	$3^-(4^+)$
11	6605(60)	

peaks of interest were separated from those of contaminants. The determinations of the energy differences are accurate to ≤ 10 keV, except for that between the 6000 and 6605 keV states for which the uncertainty is ± 50 keV, primarily due to the poor statistics and large background. The excitation energies are presented in Table I with their uncertainties.

Proton angular distributions were measured for the 11 lowest states in the range $20^\circ \leq \theta_p \leq 70^\circ$ (laboratory frame).

The ground state Q value for the (t,p) reaction on ^{36}S , based on our data, is 3838(30) keV, which implies a mass excess for ^{38}S of $-26\,843(30)$ keV. This is in good agreement with the previous mass excess measurements by Mayer *et al.*¹⁴ and Engelbertink and Olness,¹⁷ which are $-26\,863(10)$ and $-26\,858(21)$ keV, respectively.

Our results for the excitation energies of the first two excited states of ^{38}S are more precise than, but consistent with, the results of Fifield *et al.*¹³ However, our values are approximately one standard deviation lower than the values quoted by Mayer *et al.*¹⁴ A possible reason for this discrepancy is that Doppler effects were not considered by the latter authors, who employed the $^{36}\text{S}(^{18}\text{O}, ^{16}\text{O}\gamma)^{38}\text{S}$ reaction at $E(^{18}\text{O})=18$ MeV. Using a thin target they observed ^{16}O nuclei (at $\theta_p=-8^\circ$) in coincidence with γ rays detected in a Ge detector set at $\theta_\gamma=90^\circ$. (Angles are given relative to the ^{18}O beam direction.) For this geometry (recoils into vacuum) we estimate a recoil ^{38}S velocity component along the γ -detection axis (z) of $\langle \beta_z \rangle \equiv \langle v_z/c \rangle \sim 0.0035(0.0008)$. Correcting for this expected Doppler shift leads to revised transition energies of 1292(1) and 1532(2) keV, and corresponding excitation energies of 1292(1) and 2824(2) keV. The revised values are in excellent agreement with the present work.

IV. DWBA CALCULATIONS

DWBA calculations of differential cross sections were carried out using the code DWUCK4 (Ref. 18). A microscopic (t,p) form factor, with the triton represented by a Gaussian wave function with an rms radius of 1.7 fm, was used. For two-neutron transfer spin-zero transfer is

TABLE II. Optical potential parameters. A is adjusted to give each neutron a binding energy of $(Q + S_n)/2$, where Q represents the ground state Q value and S_n is half the two-neutron separation energy.

Channel	V_0 (MeV)	r_0 (fm)	a_0 (fm)	W (MeV)	r_w (fm)	a_w (fm)	W_D (MeV)	r_D (fm)	a_D (fm)	r_c (fm)
Entrance	172.7	1.16	0.7	14.8	1.65	0.806				1.25
Exit	54	1.25	0.65				48.8	1.25	0.47	1.25
Bound state	A	1.27	0.65							

strongly favored over spin-one transfer, so the total angular momentum transfer is equal to the orbital angular momentum transfer, and thus only natural parity states are populated. The two transferred neutrons were assumed to be in pure configurations. A simple shell model picture of the ^{36}S target nucleus having a closed neutron sd shell, suggests that the most likely configuration for transferred neutrons resulting in positive parity states is $(1f_{7/2})^2$. For negative parity states, it is not clear what the most likely configuration for the transferred nucleons would be; but calculations for $L=3$ and $L=5$, assuming $(1f_{7/2}1d_{3/2})$ and $(1f_{7/2}1g_{9/2})$ configurations, showed that the shape of the resulting angular distributions does not exhibit much sensitivity to the configuration assumed, within the angular range for which data are available.

The experimental angular distribution for the 0^+ ground state of ^{38}S was compared with DWBA calculations in order to choose appropriate parameters for use in the DWBA calculations for the other states. The optical potential parameters used¹⁹ are given in Table II. For the entrance and exit channels

$$V(r) = -V_0 f(x_0) - iWf(x_w) + iW_D \frac{df(x_D)}{dx_D} + V_C(r_c), \quad (1)$$

with

$$f(x_n) = \left[1 + \exp \left[\frac{r - r_n A^{1/3}}{a_n} \right] \right]^{-1}. \quad (2)$$

Here, A is the mass number of the nucleus and $V_C(r_c)$ is the Coulomb potential due to a uniformly charged sphere of radius r_c . For the bound state

$$V(r) = V_0 \left[-f(x_0) + \frac{\lambda}{45.2r} \frac{df(x_0)}{dr} \underline{L} \cdot \underline{S} \right], \quad (3)$$

with the Thomas orbit coupling strength set to $\lambda=25$.

The proton potential is the global form of Perey²⁰ with the real depth varied about the prescribed value to obtain the best fit to the ground state data. The triton potential is for 20-MeV elastic scattering on ^{40}Ca (Ref. 21).

V. ANGULAR DISTRIBUTIONS

DWBA calculations for a range of L transfers were compared with the experimental differential cross sections in order to restrict the possible spin assignments for the ^{38}S states. The experimental data are shown in Fig. 2, together with the DWBA calculations.

The calculated angular distributions for $L=1$ and $L=2$ are quite similar so a distinction between these is

difficult to make. However, from systematics for even-even nuclei, the 1295-keV first excited state in ^{38}S (denoted as 1 in Fig. 2) is almost certainly a $J^\pi=2^+$ state. Because the experimental angular distribution for the 3375-keV state (3) is so similar to that for the 1295-keV state, it is likely to be a 2^+ state also. The same argument applies for the 4955- and 5278-keV states (7,9) although there are fewer data points for the latter and the $L=3$ DWBA calculations also reproduce the data reasonably well. The angular distribution for the 5064-keV state (8) agrees well with the $L=3$ calculation but there is also some resemblance to the $L=2$ data.

The calculated angular distributions for $L=3$ and $L=4$ are again quite similar but a definite distinction can be made for the 2835-keV state (2). For this state the agreement with the $L=4$ calculation is extremely good, leading to a unique 4^+ assignment. The other states with which the $L=3$ and $L=4$ calculations show good agreement are the 4336-, 4478-, and 6000-keV states (5,6,10). Comparison of the experimental data for these states with that for the 2835-keV state (2) shows that the angular distribution for the 4336-keV state (5) is very similar, so a 4^+ assignment is preferred. Also, the $L=4$ calculation for the 4336-keV state (5) shows rather better agreement with the data than does the $L=3$ calculation, although $L=3$ cannot be ruled out. The 6000-keV state (10) has an experimental angular distribution rather different from that of the 2835-keV state (2). This leads to a preference for a 3^- assignment, although $L=4$ cannot be ruled out.

The 3690-keV state (4) has an angular distribution of less slope than all the other states. It is well represented by an $L=5$ calculation and does not show good agreement with calculations involving any other L value, although, as discussed later, local systematics and model calculations strongly favor assignment of this level as the expected 6^+ member of the $(1f_{7/2})^2$ quartet. None of the other experimental angular distributions are flat enough to show agreement with an $L=6$ DWBA calculation.

There is a significant angular momentum mismatch in the $^{36}\text{S}(t,p)^{38}\text{S}$ reaction since the partial waves which contribute to the distorted wave function in the entrance channel are of higher angular momentum than those for the exit channel. Five units of angular momentum are required for a matched condition so reactions leading to all but the 3690-keV state are mismatched. Because of this mismatch there is a comparatively large contribution to the transition matrix element from the lower angular momentum, strongly absorbed, partial waves in the entrance channel. The distorted wave function for this channel in the nuclear interior is therefore important and finite range effects may be significant. The effect of a finite range correction in the local energy approximation

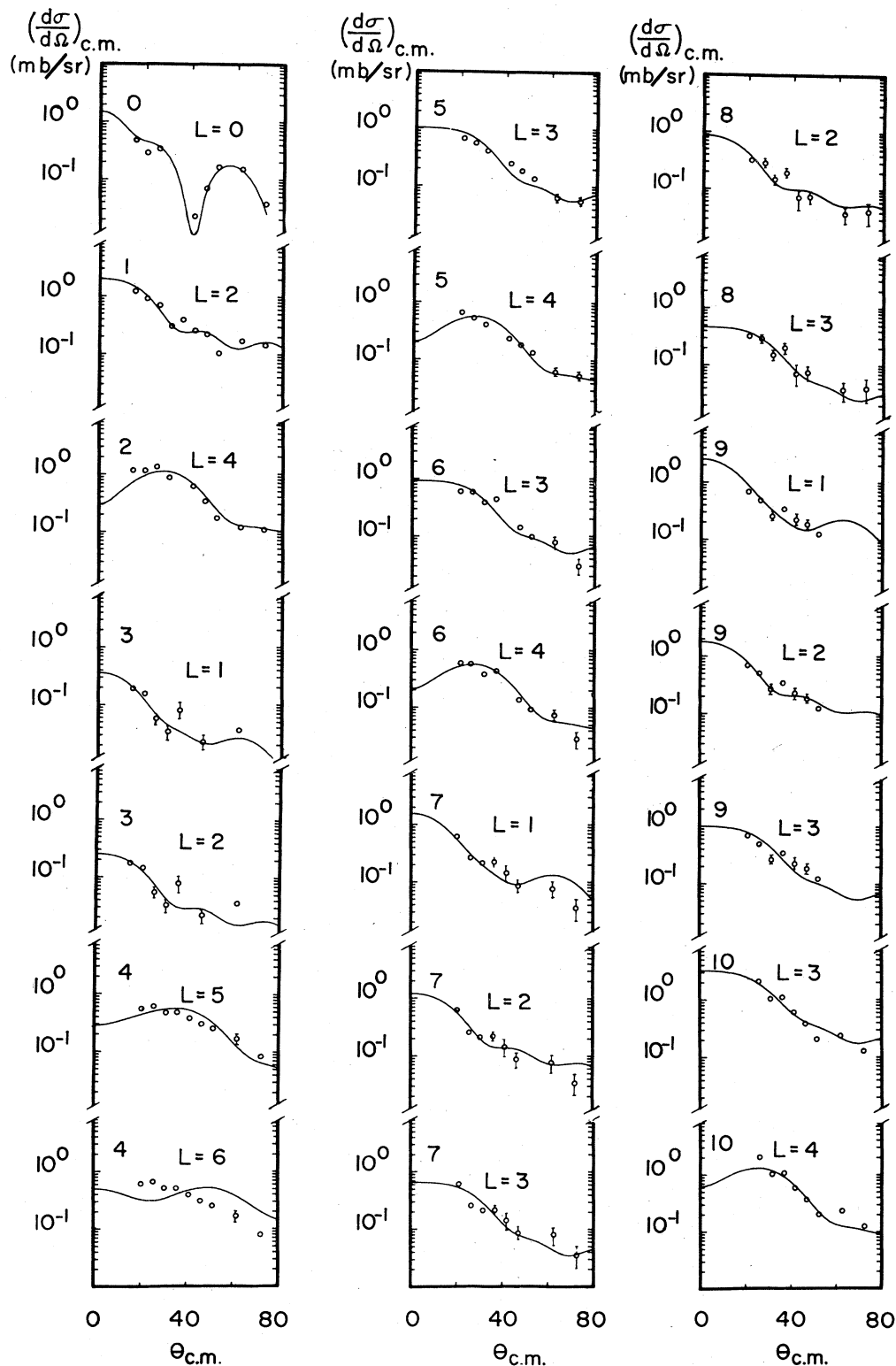


FIG. 2. DWBA calculations compared with experimental angular distributions for states populated by the $^{36}\text{S}(t,p)^{38}\text{S}$ reaction. See Table I for the state numbers and the corresponding energies.

is to reduce contributions from the wave function in the nuclear interior, and consequently, it has more effect in the case of mismatch than for the matched condition. A finite range corrected calculation was performed for the

$L=0$ ground state, for which the mismatch is greatest and the free parameter of this correction was varied to obtain the best fit to the data. This finite range correction was applied also to the 1295- and 2835-keV states and the

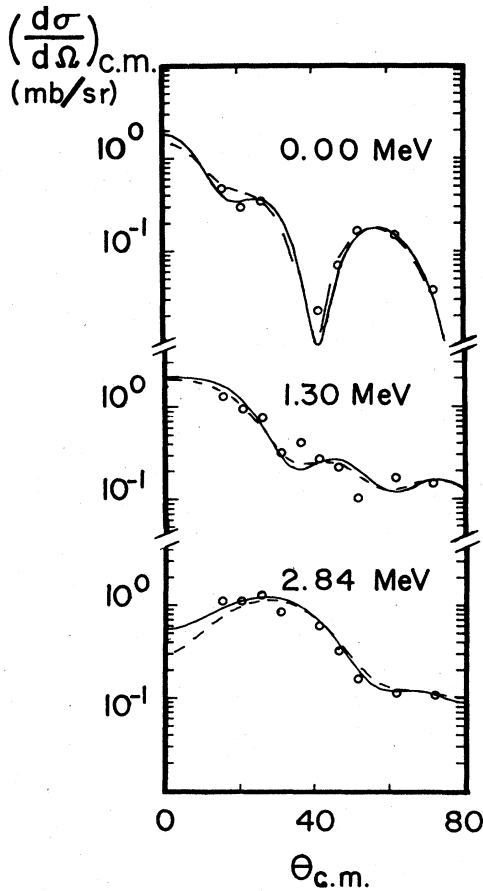


FIG. 3. DWBA calculations showing finite range corrections. (Dashed curve, uncorrected; solid curve, corrected.)

results are shown in Fig. 3. A slight improvement in the agreement with the data is observed for the $L=0$ and $L=4$ cases at the smaller angles, but overall there is not much difference, suggesting that finite range corrections are in this case not important.

VI. WEAK-COUPLING MODEL CALCULATIONS

States in ^{38}S populated strongly by the (t,p) reaction are likely to be configurations involving the two transferred neutrons in single particle states coupled to the inert ^{36}S core. One could therefore expect that states observed in the $^{36}\text{S}(t,p)^{38}\text{S}$ reaction should be similar to states populated by the (t,p) reaction in other even-even nuclei with the same neutron number as ^{38}S (Refs. 22–26).

The weak coupling method of Bansal and French²⁷ can be used to calculate the energies of particle-hole states in ^{38}S . The energy of a state with n_p particles and n_h holes is given by

$$E = -B_p - B_h - an_p n_h + b/2 [T(T+1) - t_p(t_p+1) - t_h(t_h+1)] + C, \quad (4)$$

where B_p and B_h are the binding energies of the particle and hole configurations, t_p and t_h are their isospins, and T is the isospin of the states in ^{38}S . a and b parametrize the interaction between the particle and hole configura-

tions and the Coulomb term C is zero in this case. The parameters a and b are given the values -0.3 and 2.55 MeV, respectively.²⁸

The results of the weak coupling calculation for ^{38}S are compared with experiment in Fig. 4. The measured strengths of the states are indicated relative to that for the 2835-keV state. States in ^{38}S strongly populated by the (t,p) reaction are expected to be those corresponding to two-neutron states in ^{42}Ca ; such states are indicated by the heavy lines in Fig. 4. The particle states of the calcium isotopes relevant to this weak coupling calculation were identified using the results of shell-model calculations in a $(1f_{7/2}2p_{3/2})$ configuration space.²⁹

From the shell model, the low-lying neutron states should be $(1f_{7/2})^2$ configurations giving a $0^+, 2^+, 4^+, 6^+$ sequence of levels. The ground and first two excited states in ^{38}S clearly correspond to the first three members of this sequence and have energies which agree well with the 2p-4h weak coupling levels. The overall evidence strongly suggests that the 3690-keV state is the fourth member of the quartet, particularly on account of its large (t,p) strength. The 2p-4h state predicted by the weak coupling model at 4.5 MeV corresponds to a $2^+, 4^+$ doublet in ^{42}Ca , of which only the 2^+ state is populated by the (t,p) reaction.³⁰ It is therefore thought that the ^{38}S level at 4955 keV is likely to be this 2p-4h state.

An important feature indicated by the weak-coupling model is that the $2\hbar\omega$ 4p-6h intruder states are predicted to occur higher in excitation energy in ^{38}S than the $2\hbar\omega$ states in ^{42}Ca where 4p-2h 0^+ and 2^+ intruder states are observed lower in excitation energy than the $(1f_{7/2})^2$ 4^+ state. Negative parity 3p-5h states are predicted by the weak-coupling model to occur above 4.7 MeV in ^{38}S . Possible negative-parity states are observed in this energy region.

VII. SHELL-MODEL CALCULATIONS

The nucleus ^{38}S has 22 neutrons and hence a suitable basis for shell-model calculations must involve both sd and pf shell orbits. Untruncated calculations, while possible for the sd shell alone, are clearly prohibitively large when pf orbitals are included; indeed, quite severe truncation is necessary if the matrices to be constructed and diagonalized are to be kept to manageable dimensions. The most practical single-particle basis for a nucleus such as ^{38}S is probably one in which only the $s_{1/2}$, $d_{3/2}$, $f_{7/2}$, and $p_{3/2}$ orbitals are active. Two different sets of empirical two-body matrix elements (TBME) and single-particle energies (s.p.e.) in such a basis have been proposed by Hasper³¹ for positive- and negative-parity states, respectively. These effective interactions resulted in predicted level schemes in fair agreement with the experimental data when "diagonal percentage truncation" was used.

It is well known^{32–34} that Hasper's matrix elements [derived basically from a modified surface-delta interaction (MSDI)] suffers from certain deficiencies, in particular, too much mixing between the sd and pf configurations. This can be attributed to the very small energy gap (only 1.5 MeV) between the $d_{3/2}$ and $f_{7/2}$ single particle orbits. Accordingly, Van der Poel *et al.*³² have proposed

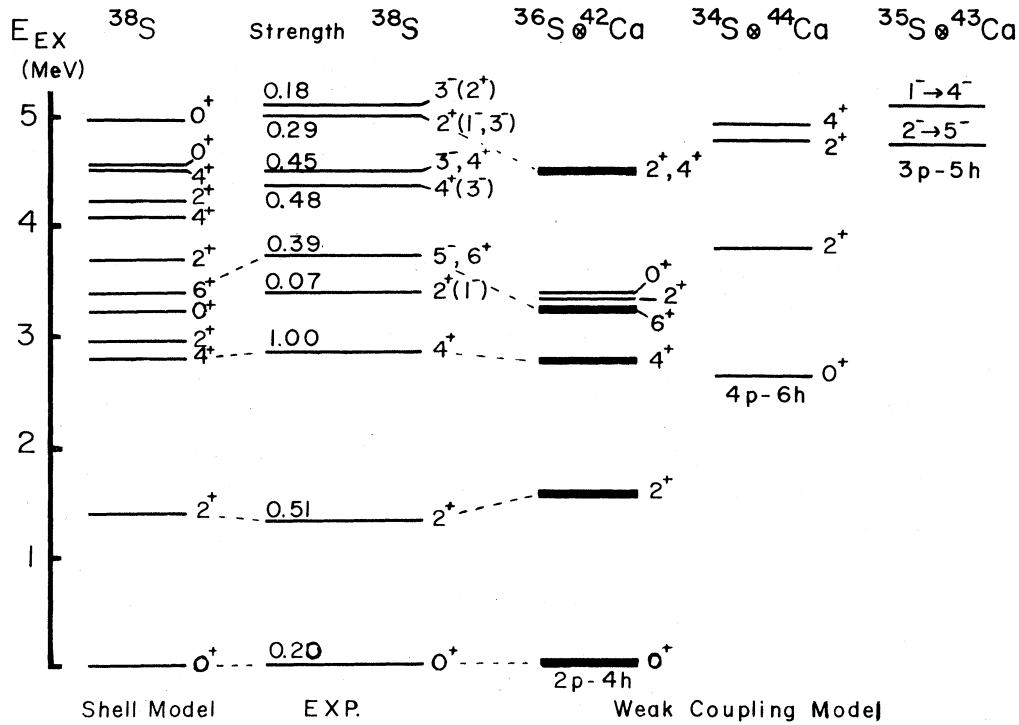


FIG. 4. Weak coupling and shell model calculations for ^{38}S . The heavy lines indicate weak coupling states derived from two particle states in ^{42}Ca which are strongly populated by the (t,p) reaction.

a new set of two-body matrix elements and s.p.e. which give better agreement for level energies and electromagnetic properties in the $A = 34-39$ nuclei.

We have carried out shell-model calculations for the ^{38}S level scheme and two-particle parentage amplitudes for use in predicting $^{36}\text{S}(t,p)$ cross sections, using the code OXBASH (Ref. 35) and both the Hasper and Van der Poel matrix elements. It was found that a simple modification of Hasper's s.p.e. gave much better agreement with the experimental results for ^{36}S , which was used as a "test case." For this calculation, a full $(s_{1/2}d_{3/2})^{8-n}(f_{7/2}p_{3/2})^n$ space was used, with $n=0,2$. Basically, the $f_{7/2}p_{3/2}$ shell orbits were moved higher up in energy relative to the $s_{1/2}d_{3/2}$ orbits. This resulted in a higher excitation energy for the 0_2^+ state and in less cross-shell mixing, as expected.

In this work, however, we only report the results of calculations using the Van der Poel *et al.* interaction³² since global predictions with this interaction are generally accepted^{33,34} to be superior to those with the Hasper matrix elements.

A. Level schemes

Calculations were done using the interaction of Ref. 32 in an $s_{1/2}d_{3/2}f_{7/2}p_{3/2}$ basis and using a variety of truncation schemes. Good agreement for the ^{38}S energy level scheme was obtained from an otherwise unrestricted $(s_{1/2}d_{3/2})^8(f_{7/2}p_{3/2})^2$ space, with the largest matrix having dimension 26 for $J^\pi=2^+$, $T=3$. An $(s_{1/2}d_{3/2})^7(f_{7/2}p_{3/2})^3$ configuration was used for negative parity levels. Calculations were also performed in spaces where two additional sd -shell particles were promoted to

the pf shell (i.e., including $2\hbar\omega$ excitations). To keep the size of the matrices down to manageable dimensions, the distributions of the ten "valence" nucleons amongst the available orbitals had to be restricted in some fashion. These much larger calculations, however, did not result in appreciably improved level schemes or parentage amplitudes; thus, we only report results for the small basis discussed above.

The calculated spectra are shown in Fig. 4, and are in generally good agreement with those experimentally observed. In addition, they are in qualitative agreement with the predicted $2p$ - $4h$ states of the weak coupling model. Predicted negative parity levels are not shown in Fig. 4, but start at around 5.5 MeV excitation. The only natural parity state with no experimental counterpart is the second 0^+ state; as will be shown in the next section, this can be attributed to the structure of this state.

B. Parentage amplitudes

The comparison of experimental (t,p) cross sections with theoretical cross sections calculated using parentage amplitudes from shell model wave functions is a sensitive test, not only of the magnitudes of the various components, but also of their phases. The DWBA cross section does not easily factorize into convenient "structure-dependent" and "structure-independent" terms, but is the square of a coherent sum of multiples of individual structure- and kinematical amplitudes. These structure-dependent amplitudes are proportional to two-nucleon parentage amplitudes: reduced matrix elements of products $a_i^\dagger a_j^\dagger$ of nucleon creation operators between the ^{36}S ground state wave function and the various ^{38}S excited

TABLE III. Two-particle parentage amplitudes and enhancement factors.

Excitation energy (keV)	J^π	Transferred configuration	Two-particle parentage amplitude	Enhancement factor
0	0^+	$2s_{1/2}^2$	0.1633	0.65
		$1d_{3/2}^2$	0.3750	
		$1f_{7/2}^2$	-0.6788	
		$2p_{3/2}^2$	-0.3513	
1295	2^+	$2s_{1/2}1d_{3/2}$	0.0481	0.72
		$1d_{3/2}^2$	-0.0338	
		$1f_{7/2}^2$	0.4024	
		$1f_{7/2}2p_{3/2}$	-0.4451	
		$2p_{3/2}^2$	0.1634	
2835	4^+	$1f_{7/2}^2$	-0.5651	1.2
		$1f_{7/2}2p_{3/2}$	0.3785	
3204	0^+	$2s_{1/2}^2$	-0.0269	
		$1d_{3/2}^2$	-0.0457	
		$1f_{7/2}^2$	0.2190	
		$2p_{3/2}^2$	-0.0012	
3690	6^+	$1f_{7/2}^2$	0.7570	2.1

state wave functions.

From the shell-model wave functions, we have obtained these two-nucleon parentage amplitudes for the lowest states in ^{38}S , for which a correspondence between experimental and predicted levels is possible. These parentage amplitudes, *modified where necessary to conform to the phase convention used in DWUCK4*, are listed in Table III. The excitation energy assigned to the second 0^+ state in Table III is that given by the shell model.

In order to compare experimental and predicted cross sections, DWBA calculations are commonly normalized³⁶ via

$$\sigma_{\text{exp}} = N\epsilon\sigma_{\text{DWBA}}, \quad (5)$$

where N is the "normalization constant," determined from a global comparison between experiment and DWBA for many nuclei, and ϵ is the so-called enhancement factor. The factor ϵ is a measure of how well the experimental data are described by the shell-model calculation, since the (t,p) normalization and Q -value effects have been removed. Thus, ϵ values are truly meaningful only for those levels for which unique shell-model counterparts can be assigned. An "exact" prediction would produce $\epsilon=1$.

When each calculated angular distribution is independently normalized to the data, the product $N\epsilon$ can be obtained from Eq. (5). N appears^{36,37} to depend on the DWBA parameters used in a particular calculation; however, $N \sim 218$ is not unreasonable.³⁶ The ϵ values deduced for the observed states are given in Table III as well. The agreement obtained (i.e., ϵ values within a factor of 2 of unity) indicates that the present shell-model wave functions do indeed give a good quantitative description of the

structure of the low-lying levels. DWBA calculations using the parentage amplitudes for the second 0^+ state give differential cross sections less than 1.5×10^{-4} mbsr⁻¹. The smallest differential cross section measurable under the conditions of this experiment is estimated to be 2.0×10^{-2} mbsr⁻¹, so the nonobservation of this state is consistent with the shell-model predictions.

Hence, this first shell-model calculation for ^{38}S has been reasonably successful. Data such as those obtained in the present work, for nuclei in which both sd and pf shells are active, should allow further refinements to be made to the TBME. It is not too much to hope that in the future, enough such data will become available to permit the determination of an effective interaction in this mass region comparable to the enormously successful "universal" sd -shell interaction of Wildenthal.³⁸

VIII. CONCLUSIONS

The $^{36}\text{S}(t,p)^{38}\text{S}$ reaction has been used to identify several low-lying levels in ^{38}S , a $T_z=3$ nucleus about which very little was previously known. Comparison of the experimental angular distributions with DWBA calculations provides spin assignments, or significant restrictions, for many of the states identified. Comparison of the ^{38}S levels found in this experiment with states predicted by the weak coupling model reveals states of 2p-4h nature including those of two-neutron $(1f_{7/2})^2$ configuration. In particular, the ground state and first two excited states are identified as the $0^+, 2^+, 4^+$ members of this configuration. Shell-model calculations of ^{38}S energy levels and transition strengths are found to be in quite good agreement with the properties of the experimental levels.

ACKNOWLEDGMENTS

This research was supported in part by the Natural Sciences and Engineering Research Council of Canada and in part by the U.S. Department of Energy, Division of Basic Energy Sciences under Contract No. DE-AC02-76CH00016 with the Associated Universities, Inc. (BNL), and No. DE-AC05-84OR21400 with the Martin Marietta Energy Systems (ORNL).

- ¹J. W. Olness, W. R. Harris, A. Gallmann, F. Jundt, D. E. Alburger, and D. H. Wilkinson, *Phys. Rev. C* **3**, 2323 (1971).
- ²A. M. Baxter and S. Hinds, *Nucl. Phys.* **A211**, 7 (1973).
- ³D. J. Crozier, H. T. Fortune, R. Middleton, and S. Hinds, *Phys. Rev. C* **17**, 455 (1978).
- ⁴J. G. Pronko and R. E. McDonald, *Phys. Rev. C* **6**, 2065 (1972).
- ⁵G. Guillaume, B. Rasteger, P. Fintz, and A. Gallmann, *Nucl. Phys.* **A227**, 284 (1974).
- ⁶E. A. Samworth and J. W. Olness, *Phys. Rev. C* **5**, 1238 (1972).
- ⁷B. L. Cohen and R. Middleton, *Phys. Rev.* **146**, 748 (1966).
- ⁸S. Hinds and R. Middleton, *Nucl. Phys.* **A92**, 422 (1967).
- ⁹B. L. Cohen, C. L. Fink, J. B. Moorhead, and R. A. Moyer, *Phys. Rev.* **157**, 1033 (1967).
- ¹⁰R. Chapman, S. Hinds, and A. E. MacGregor, *Nucl. Phys.* **A119**, 305 (1968).
- ¹¹W. Darcey, R. Chapman, and S. Hinds, *Nucl. Phys.* **A170**, 253 (1971).
- ¹²R. F. Casten, E. R. Flynn, Ole Hansen, and T. J. Mulligan, *Phys. Rev. C* **4**, 130 (1971).
- ¹³L. K. Fifield, M. A. C. Hotchkis, P. V. Drumm, T. R. Ophel, G. D. Putt, and D. C. Weissner, *Nucl. Phys.* **A417**, 534 (1984).
- ¹⁴W. A. Mayer, W. Henning, R. Holzworth, H. J. Körner, A. Korschinek, W. U. Mayer, G. Rosner, and H. J. Scheerer, *Z. Phys. A* **319**, 287 (1984).
- ¹⁵C. E. Thorn, J. W. Olness, E. K. Warburton, and S. Raman, *Phys. Rev. C* **30**, 1442 (1984).
- ¹⁶S. Raman, W. Ratynski, E. T. Journey, M. E. Bunker, and J. W. Starner, *Phys. Rev. C* **30**, 26 (1984).
- ¹⁷G. A. P. Engelbertink and J. W. Olness, *Phys. Rev. C* **3**, 180 (1971).
- ¹⁸P. D. Kunz, DWUCK4, 1974 (unpublished).
- ¹⁹E. R. Flynn, Ole Hansen, R. F. Casten, J. D. Garrett, and F. Ajzenberg-Selove, *Nucl. Phys.* **A246**, 117 (1975).
- ²⁰F. G. Perey, *Phys. Rev.* **131**, 745 (1963).
- ²¹E. R. Flynn, D. D. Armstrong, J. G. Beery, and A. G. Blair, *Phys. Rev.* **182**, 1113 (1969).
- ²²R. Middleton and D. J. Pullen, *Nucl. Phys.* **51**, 77 (1964).
- ²³J. H. Bjerregaard, Ole Hansen, O. Nathan, R. Chapman, S. Hinds, and R. Middleton, *Nucl. Phys.* **A103**, 33 (1967).
- ²⁴J. H. Bjerregaard, Ole Hansen, O. Nathan, R. Chapman, S. Hinds, and R. Middleton, *Nucl. Phys.* **A139**, 710 (1969).
- ²⁵D. C. Williams, J. D. Knight, and W. T. Leland, *Phys. Rev.* **164**, 1419 (1967).
- ²⁶R. F. Casten, E. R. Flynn, J. D. Garrett, S. Orbesen, and O. Hansen, *Phys. Lett.* **43B**, 473 (1973).
- ²⁷R. K. Bansal and J. B. French, *Phys. Lett.* **11**, 145 (1964).
- ²⁸A. Bernstein, *Ann. Phys. (N.Y.)* **69**, 19 (1972).
- ²⁹P. Federman and S. Pittel, *Nucl. Phys.* **A155**, 161 (1970).
- ³⁰P. M. Endt and C. Van der Leun, *Nucl. Phys.* **A310**, 1 (1978).
- ³¹H. Hasper, *Phys. Rev. C* **19**, 1482 (1979).
- ³²C. J. Van der Poel, G. A. P. Engelbertink, H. J. M. Aarts, D. E. C. Sherpenzeel, H. F. R. Arciszewski, and B. C. Metsch, *Nucl. Phys.* **A373**, 81 (1982).
- ³³C. J. Van der Poel, G. A. P. Engelbertink, H. F. R. Arciszewski, P. C. N. Crouzen, J. W. De Vries, E. A. J. M. Offermann, and E. J. Evers, *Nucl. Phys.* **A394**, 501 (1983).
- ³⁴G. J. L. Nooren, H. P. L. De Esch, and C. Van der Leun, *Nucl. Phys.* **A423**, 228 (1984).
- ³⁵B. A. Brown, A. Etchegoyen, W. D. M. Rae, and N. S. Godwin, OXBASH, 1984 (unpublished).
- ³⁶J. F. Mateja, L. R. Medsker, C. P. Browne, J. D. Zumbro, H. T. Fortune, R. Middleton, and J. B. McGrory, *Phys. Rev. C* **23**, 2435 (1981).
- ³⁷D. L. Watson, M. A. Abouzeid, H. T. Fortune, L. C. Bland, and J. B. McGrory, *Nucl. Phys.* **A406**, 291 (1983).
- ³⁸B. H. Wildenthal, in *Progress in Particle and Nuclear Physics*, edited by D. Wilkinson (Pergamon, New York, 1984), Vol. 11, p. 5.